Study of the implementation of SPIF as a Reshaping strategy in terms of formability and accuracy performance

Omer Zaheer[a], Giuseppe Ingarao [a*], Rosa Di Lorenzo [a], Livan Fratini [a]

[a] Department of Engineering, University of Palermo, Viale delle Scienze, Palermo, 90128, Italy

* Corresponding author: Giuseppe Ingarao. E-mail address: giuseppe.ingarao@unipa.it

Abstract. The adaption of Circular Economy strategies has become increasingly necessary in current times. Researches need to be addressed on finding alternative processes or the modification of the existing processes in order to reprocess End-of-life (EoL) components, and consequently recover both materials and their functions. This research paper focuses on the use of Single Point Incremental Forming (SPIF) process for the Reshaping of sheet metal EoL components. Uniaxial and Biaxial pre-straining was performed on AA5754 sheets to imitate an End-of-Life component, and SPIF operations were carried out so as to obtain reshaped components. In previous works the authors have proven the technical feasibility of the said approach. The present work is focused on analyzing the possible variation in formability as well as in geometrical accuracy of SPIF process when utilized to reform components. An experimental campaign involving the variation of the pre-straining levels as well as the type (uniaxial and biaxial) was developed and the resulting formability and geometrical accuracy of the subsequent SPIF operations were then analyzed. Results showed that SPIF is a perfect candidate as Reshaping process. In fact, a very limited reduction in formability as well as the no worsening in geometrical accuracy performance was observed on the different pre-straining paths here analyzed.

Keywords: Circular Economy, Sustainability, Reshaping; SPIF; formability; accuracy.

1 Introduction

The Circular Economy paradigm has become increasingly necessary to be implemented for moving towards a better future. The anthropogenic environmental impact has by now become an imminent issue to be dealt with. Materials production industries contribute to almost 8% of total global energy demand, with a high probability of an increase in the succeeding years caused by the decrease in ore grade [1]. At the same time, it was also brought to light that, materials production processes have been one of the major contributors to yearly CO_2 emissions accounting for about 25% of the global CO_2 emissions, of which, the aluminum industry in the past two decades has had a significant increased contribution to the CO_2 emission, contributing up to 10% of the total industrial emissions [2]. Instilling the circular economy concept may help in the reduction of the environmental impact of materials production. Different strategies, as proposed by Tolio et al. [3], include intense product usage, repair and upgradation of parts, component re-use or remanufacturing, and open/closed loop recycling. The implementation of these strategies may successfully contribute towards the reduction of the environmental impact of raw materials production. So far, various recycling processes have been suggested in literature such as the development of solid state recycling processes for light alloys recycling [4] and especially in cases of aluminum alloys. These approaches have proved to lower the environmental impact of recycling [5, 6, 7]. In a framework suggested by Cooper and Allwood [8], four main strategies have been suggested for metals, two of them rely on superficial reconditioning and the product/component are reused either for the same type of function (in the case of Relocate) or for a less demanding use (in case of Cascade).

On the other hand, the remaining two imply that "The component(s) undergo extensive reconditioning" and are termed as: 1) Remanufacturing, which involves the inspection, disassembly, re-drilling, and metallic spraying/thermal techniques as the process to be applied (typical remanufacturing applications for metals concern engines and manufacturing dies [9]); and the second 2) Reform/Reshape: where manufacturing strategies (additive or subtractive) are applied to attain a new, more useful, geometry by the reprocessing of the returned End-of-Life (EoL) component by changing its shape. Consequently, the main principle of this research focuses on turning an EoL product/component directly into a reusable material or, better yet, into a different product/component. Regarding metal wastes, recycling is still one of the most applied strategy due to the benefits of its application such as, environmental, technological and economic advantages.

Without any doubt, adapting a more virtuous circular economy strategy has become an urgency through methods such as product/component reuse. Apart from the fact that the circular economy strategies allow the keeping of material in the consumption cycle, reuse strategies would also permit to recover part/component functions from the EoL components. In this regard, the manufacturing research community plays a very crucial role towards the formulation of new strategies/processes or to rethink conventional processes to be applied as circular economy enablers. While the Remanufacturing approach has been explored numerous times by the scientific community [10], the Reshaping strategy on the other hand hasn't yet been explored in depth so far. Currently a major part of the scientific work is focused on the application of Additive Manufacturing, often coupled with machining processes, for repair purposes as well as for changing of the EoL geometry [11, 12]. The strategy of employing forming processes with the intent of keeping material and functions through Reshaping, has so far been explored in a limited number of scientific works.

A research proposing the idea of re-rolling steel components recovered from vessels into semi-finished products such as plates and bars was presented by Tilwankar et al. [13]. Brosius et al. [14] proposed the idea of Reshaping an End-of-Life (EoL) automotive engine-hood into a rectangular sheet metal component utilizing the sheet hydroforming process. In another research, Takano et al. [15] proposed a strategy for the Reshaping of a previously bent sheet, by first flattening it and eventually performing an incremental forming step. Reshaping was also performed on magnesium based sheet components through super plastic forming in a study performed by Abu-Farha and Khraisheh [16]. These works, though give an insight of the possible ground breaking innovation of the Reshaping approach, they are still in the preliminary stages and the potential of forming process in this new domain still has much to still be explored. In a more recent study Ingarao et. al. [17] successfully reshaped sheet metal based EoL components through Single Point Incremental forming (SPIF). Specifically, SPIF was applied on a Deep-Drawn (DD) square shaped part in order to give it a new shape. The authors have also proved the effectiveness of SPIF based reshaped approach by comparing it with conventional stamping based reshaping approaches. Results revealed that SPIF outperformed conventional forming processes, as proved to be the only approach leading to new/reshaped component [18].

In SPIF processes, the part is formed in a stepwise manner incrementally by means of a generic tool stylus which is Computer Numerically Controlled. The sheet is clamped by the means of a non-workpiece-specific clamping system. This process is highly flexible as no tooling is required to get the desired geometry, as a matter of facts the shape is given by the numerically controlled tool path.

Also, the authors in another research paper [19] analyzed the geometrical deviation caused by SPIF process on the Depp Drawn part (in the zones not worked on by SPIF process during Reshaping). Actually, although SPIF process is characterized by low forming loads, some distortions actions on the EoL parts are still applied and geometrical deviation may occur. That research revealed that a limited distortion on the vertical wall of the DD part may occur but it can be controlled and minimized by a proper process and geometrical parameters selection.

Besides the technical feasibility, the authors also presented the fact that the Reshaping approach was a more energy efficient one when put into comparison alongside conventional and solid state recycling techniques [20].

In most cases, the EoL components comprise of localized thinning areas, characterizing them as highly heterogeneous, this in turn leaves a good proportion of the component which undergoes limited deformation. These lesser deformed zones contain a decent amount of residual formability and Reshaping can be performed utilizing almost the entire original formability. SPIF has been widely proven to be a flexible process characterized by a local forming action, whilst having an enhanced formability [21]. These advantageous characteristics of SPIF result from the unique process mechanics of which the process is comprised [22, 23, 24]. Even though the SPIF process comprises of forming loads of low magnitudes [25, 26], geometrical distortions actions during the Reshaping of EoL parts still do tend to occur [27, 28, 29]. A state-of-the-art and prospects of the SPIF process can be found in a review paper developed by Duflou et al. [30]

An approach set on the identification of process windows and the influence of the adapted process parameters on the formability and accuracy of Reshaping is much needed. So far the research in this direction has been limited, the authors formulated the present research in order to better understand the influence of different pre-straining levels on the formability as well as on the geometrical accuracy of SPIF as used as Reshaping process. So far the change in the formability of the SPIF, when used as a Reshaping tool, hasn't been studied in depth. Lora et.al. [31] in a research, explored the change in SPIF formability when used as a hybrid process, i.e. is being coupled along with stretch forming, i.e. SPIF was performed on the part, right after it's stretch forming while it was still held clamped on the stretch forming system. In their study the authors concluded that the pre-straining directly influenced the occurring deformations in the formed parts, i.e., higher deformations resulted in a high amount of residual hardening of the parts.

The present paper wants to analyze two main aspects of SPIF when used for Reshaping purposes, namely: the formability and the geometrical accuracy. Concerning the geometrical accuracy, in this paper the aim is to analyze the geometrical accuracy on the SPIFed part of the reshaped components. Overall, the research question the authors want to address is: are formability and geometric accuracy performance of SPIF affected by primary processes (pre-straining/ Deep Drawing) when used for Reshaping purpose? To answer this question, some pre-straining paths (mimicking EoL components conditions) were implemented, SPIF operations were performed on these sheets and the related formability performance and geometrical accuracy were compared to those of conventional SPIF operations developed on flat brand new sheet (with no pre-straining). With this motivation this paper presents the results of a wide experimental campaign with varying pre-restraining kind and level. The main aim is to better characterize the SPIF as Reshaping process and lay the ground towards the industrial applicability of such an approach.

2 The proposed approach

The research was formulated for having an insight on the influence of pre-straining on the formability of SPIF, while being utilized as a Reshaping strategy. The proposed study focuses on understanding the limits up to which SPIF as a Reshaping strategy of End-of-Life components may be used, in light of the effects of pre-straining on the new part geometry. This concept has, so far, been less explored by the scientific community and the research objective may shed light on the possibilities of recovering of large sheet metal components from EoL products and directly giving them a new shape through SPIF process. For example, extracting a portion of sheet metal from the hood of a car and imparting it a new shape via SPIF. Since in the case of a sheet taken from a hood of a car, residual deformations will be present due to its initial forming into a hood, the Reshaping may successfully be performed using a flexible forming process. EoL components usually consist of localized thinning areas (resulting from the original forming processes), leaving a decent portion of the component with limited deformation. These zones with comparatively lesser deformation are the main focus of interest for the purpose of the Reshaping, permitting the utilization of almost the entire original formability. A simplified objective of the research approach is illustrated in fig. 1.

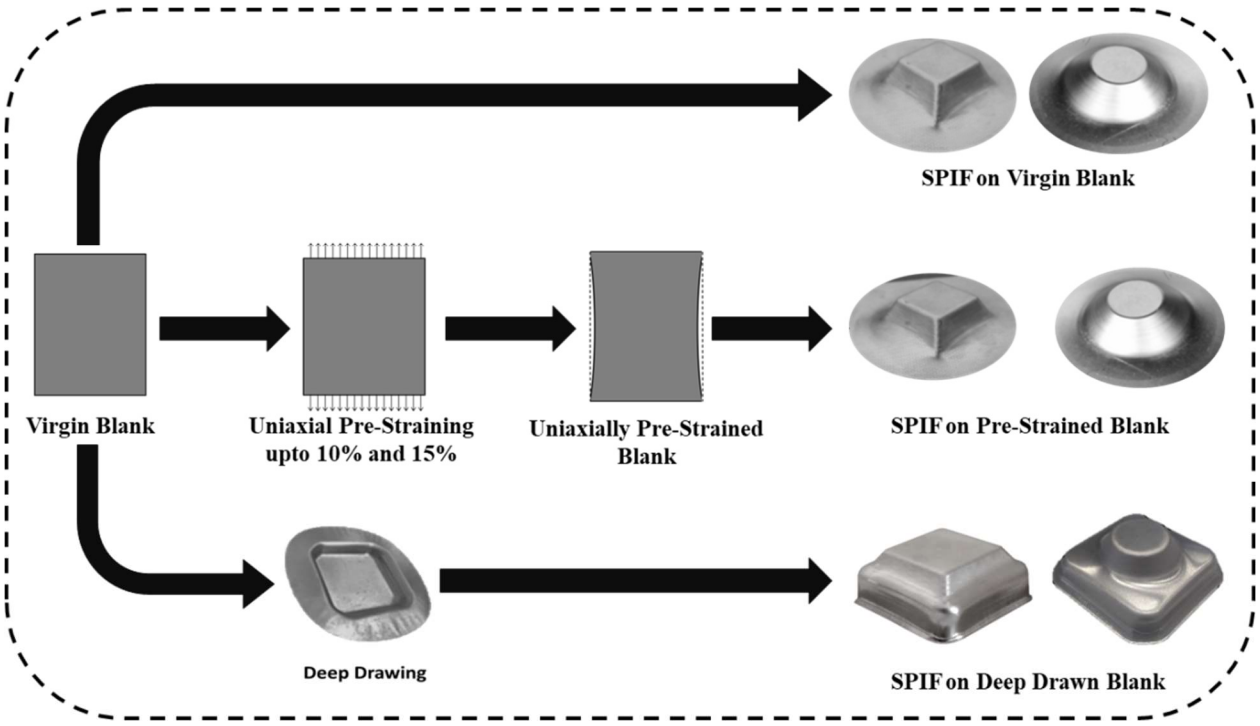

Fig. 1. The proposed processes chains for characterizing Reshaping

To achieve the research objectives, the authors turned a virgin blank into an EoL component by imparting it deformations. Two different levels of uniaxial pre-straining and a biaxial pre-straining (deep drawing) were considered as primary processes to resemble an EoL component. For the Reshaping of the components, truncated pyramid and cone were formed onto the deformed parts via the SPIF process. The EoL component obtained after deep drawing was reshaped by performing SPIF process on the base of the component along the direction same as that of deep drawing.

3 Materials and Methods

In order to proceed with the research objectives, an experimental campaign was designed for tests to be performed on an aluminum alloy sheet AA5754 having a thickness of 0.5mm. For the pre-straining step of the experimental campaign, a Galdabini Quasar 500 hydraulic press was used to perform the uniaxial and biaxial straining of the sheets. The sheets were subjected to two different levels of uniaxial strain, i.e., stretching of the blank up to 10% and 15% of its original length. For the performance of biaxial straining, deep drawing process was performed to obtain a square cup 16mm deep. The geometrical parameters for the deep drawing and SPIF processes are illustrated in figure 2. For all the pre-straining tests a constant punch velocity of 1mm/s was used. The SPIF based Reshaping step of the experimental campaign was performed on a 4 axes CNC milling machine a tool with a high-speed steel based 4 mm diameter. Helical tool paths with a 0.1 mm descent was applied for all the processes. A fee rate equal to 400 mm/min was used, no rotational speed was programmed and the forming tool was set free to rotate. The contact zone was lubricated by using hydraulic oil. In order to hold the specimens firmly in place, during the SPIF process, a dedicated clamping system was (as in figure 2a) used. The authors chose to take into account the maximum formable angle (α max) via the SPIF process as an indicator of the variation in formability resulting from different types of pre-straining. For both truncated cone and pyramid the angle used for identifying the α max is reported in figure 2 c and d (α^0); specifically, the higher the α max is the more formable is the analyzed material. The campaign was divided into 2 case studies, incremental forming of a truncated cone and pyramid, the dimensions of the deep drawn part and the SPIFed shapes are illustrated in figure 2 (b, c and d).

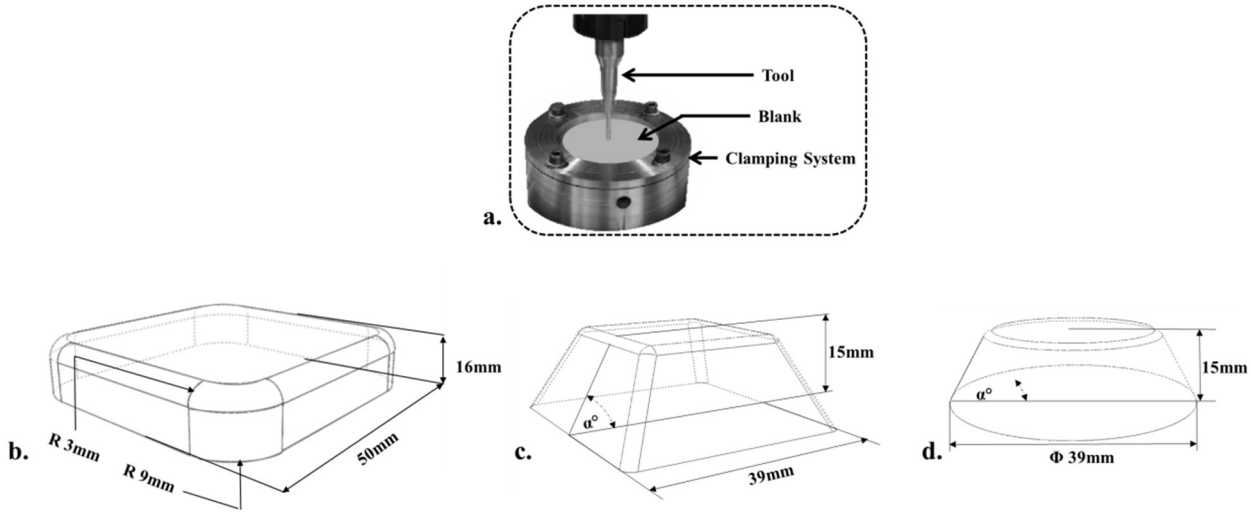

Fig. 2. Experimental setup and part dimensions; (a) SPIF setup and clamping system; (b) square cup geometry; (c) truncated pyramid geometry, (d) truncated cone geometry.

3.1 Methodology for α max calculation

The primary objective of this research was to investigate the maximum formable angle (α max) through the SPIF process, for the forming of truncated cone and pyramid. It is worth remarking that the easiest way to express the formability of SPIF is the characterization of the maximum wall angle before failure occurs [32]. This maximum angle is dependent on the material type, sheet thickness and process parameters such as tool radius, step down, feed rate, local temperature of the sheet, etc.

In the present study, SPIF was performed onto a virgin blank to form the selected shapes while increasing the forming angle by half a degree every time a non-fractured part was obtained. As soon as a fractured part was obtained, the preceding angle was ascertained as the α max corresponding to the shape being formed. With the aim to have a decent consistency in the findings, the SPIF process at the obtained α max was performed thrice. After the identification of α max for both the case studies, the research proceeded towards studying the influence of different types of pre-straining on the SPIF formability. The virgin blank received underwent two different types of pre-straining. The uniaxial pre-straining step was performed on the Galdabini Quasar 600, where the blank was stretched, with the help of a pneumatic clamping jaws, up to 10% and 15% of its original length. The biaxial pre-straining was also performed on the Galdabini Quasar 600 hydraulic press, using a dedicated system mounted on to the press to obtain a square cup. After the pre-straining steps, the blanks were cut accordingly so as to clamp it for the following SPIF step. The process for α max identification was performed again on the pre-strained blanks. After determining the α max corresponding to each pre-straining condition, the next step of the experimental campaign was the measurement of the occurring deformations in each of the parts when undergoing SPIF at α max + 0.5°. In order to do so, a pattern of circles 1.5mm in diameter, having a depth of 0.05mm, were laser incised on the sheets before they underwent the pre-straining and later SPIF. In figure 3 an example of fractured sample is reported for the truncated cone case study.

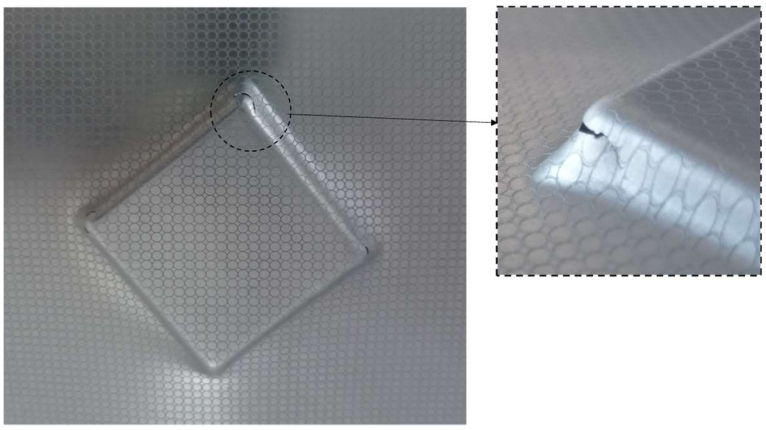

Figure 3. Example of applied circle pattern with fracture occurrence at pyramid edge.

For the correct identification of the pre-straining level in the case of DD, the process chain was numerically simulated. The numerical approach was adapted to track back the pre-straining level corresponding to the fractured zone, i.e. upon identifying the fracture zone in the deep drawn part, after its Reshaping, the exact pre-straining levels were also measured experimentally. The entire process chain was numerically simulated using the explicit code LS-DYNA, and springback analyses were carried out with its implicit solver after each forming simulation. In other words, a four steps approach was undertaken, two explicit steps for DD and SPIF, one implicit approach after the explicit simulation. According to previous experiences on these numerical models [33], a full integrated quadrilateral shell element with seven integration points along thickness was utilized. A Coulomb model was considered for frictional actions and the Barlat–Lian constitutive model with an isotropic work hardening was utilized. The numerical model for reshaping purpose on the same material had been already validate by the authors in a previous research [17]. The minor strain maps for the DD and related Reshaped components (fracture conditions for truncated pyramid) are reported in figure 4a end 4b, respectively. In this figure the fracture area (occurring during SPIF operations) in the DD and in the Reshaped parts is highlighted, the related major and minor strains are also reported.

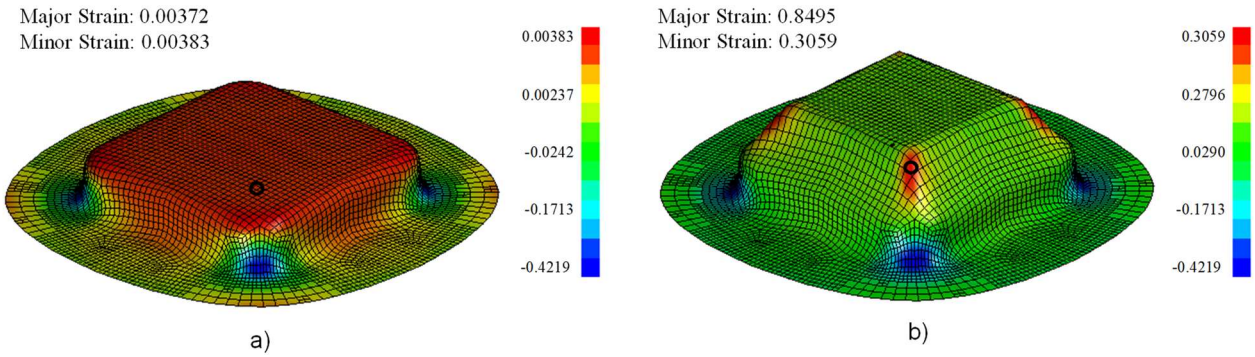

Fig. 4. Minor strain maps along with major and minor strain values of fracture area for the DD a) and related reshaped component (fracture conditions) b).

3.2 Methodology for the geometrical accuracy analysis

In order to study the variation in the geometrical accuracy of parts reshaped through SPIF, corresponding to different types of pre-straining levels, comparisons of geometries after Reshaping were developed. In particular, the geometries obtained after the SPIF process were compared to a reference CAD model of a truncated cone and pyramid designed having the same geometrical attributes. In order to analyze if the extent of deformation of SPIF affects the accuracy of the Reshaping process, the two angles selected for the shapes to be formed were: a lower value ($\alpha = 45°$); and higher value ($\alpha = 65°$) for both the truncated cone and the pyramid. In table 1 the developed experimental campaign is reported. In order to have a consistency in the results, three replications of each experiment ID were performed. Throughout the experimental campaign, SPIF was performed following a helical tool path with a 0.3 mm descent applied for each spire. The geometries of experimental parts were acquired with the help of a photo acquisition system, 'Steinbichler COMET' 3D Scanner. The acquired geometries were then analyzed through 'GeoMagic Control X' software. This way the CAD model (used as reference) along with the reshaped part geometries were aligned and compared.
To be more specific, the used 3D scanner is based on structured light technique using fringe projection with an accuracy equal to 0.015 mm. The output of the scanning process is the STL file of acquired geometry that is further processed for analysing the shape accuracy of the reshaped components: for each ID of table 1, geometric deviations occurring in the reshaped components were quantified by comparing the obtained (acquired) geometry to that of a CAD model having the shape and the angle as reported in table 1. The comparison was performed using 3D quality control and dimensional inspection software, 'Geomagic Control X'. Within Geomagic Control X environment it is possible to optimize the alignment of two surfaces by the application of the iterative closest point algorithm which minimises the sums of squares of distances between the sample pairs.

The Maximum Deviation and the Root Mean Squared (RMS) error were recorded as metric for geometric accuracy quantification. The recorded data were then analyzed through the ANOVA (Analysis of Variance) statistical tool. ANOVA is a statistical tool which allows the detection of differences between the means of different experimental group. ANOVA is formulated in experimental designs with a parametric numerical outcome, which is a variable dependent on one, or multiple, experimental groups (independent variables) [34]. The analysis was performed utilizing MINITAB statistical analysis software considering a significance level of $\alpha = 0.05$. The results obtained have been discussed in section 4. Table 1 details all the experimental tests performed for the two case studies and figure 5 shows some of the results obtained corresponding to IDs 6, 3, 8, 13, 10 and 16.

Table 1. Experimental Campaign.

Case Study	Part ID	Angle	Blank pre-straining Level
CONE	1	45°	Virgin
	2	45°	Uniaxial pre-strained 10%
	3	45°	Uniaxial pre-strained 15%
	4	45°	Deep Drawn Blank
	5	65°	Virgin Blank
	6	65°	Uniaxial pre-strained 10%
	7	65°	Uniaxial Pre-strained 15%
	8	65°	Deep Drawn
PYRAMID	9	45°	Virgin
	10	45°	Uniaxial Pre-strained 10%
	11	45°	Uniaxial Pre-strained 15%
	12	45°	Deep Drawn
	13	65°	Virgin
	14	65°	Uniaxial Pre-strained 10%
	15	65°	Uniaxial Pre-strained 15%
	16	65°	Deep Drawn Blank

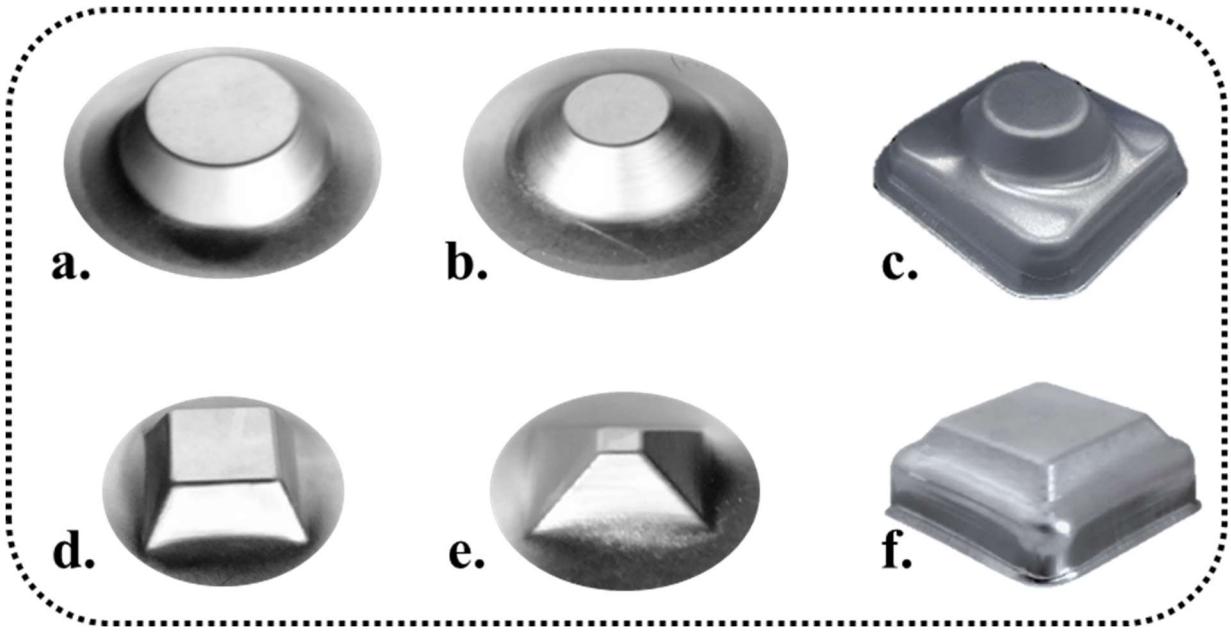

Fig. 5 Obtained parts with the part IDs: a) 6; b) 3; c) 8; d) 13; e) 10; f) 16.

4 Results

4.1 α max determination

The obtained values of α max corresponding to the different levels of pre-straining for both the case studies is reported in figure 6. As far as the reshaped samples for the cone case study are concerned, the maximum obtainable value was 68° for the virgin blank, with a decrease of 1° moving from the virgin blank conditions up to the uniaxial pre-straining of 15% and deep drawing. Whereas, in the pyramid case study the same trend was seen, with an α max of 67.5° for the virgin blank. The results show that, even though the SPIF formability decreases for the cases with pre-straining (Uniaxial 10%, 15% and Deep drawing), the difference is minimal and the Reshaping through SPIF could still be performed successfully.

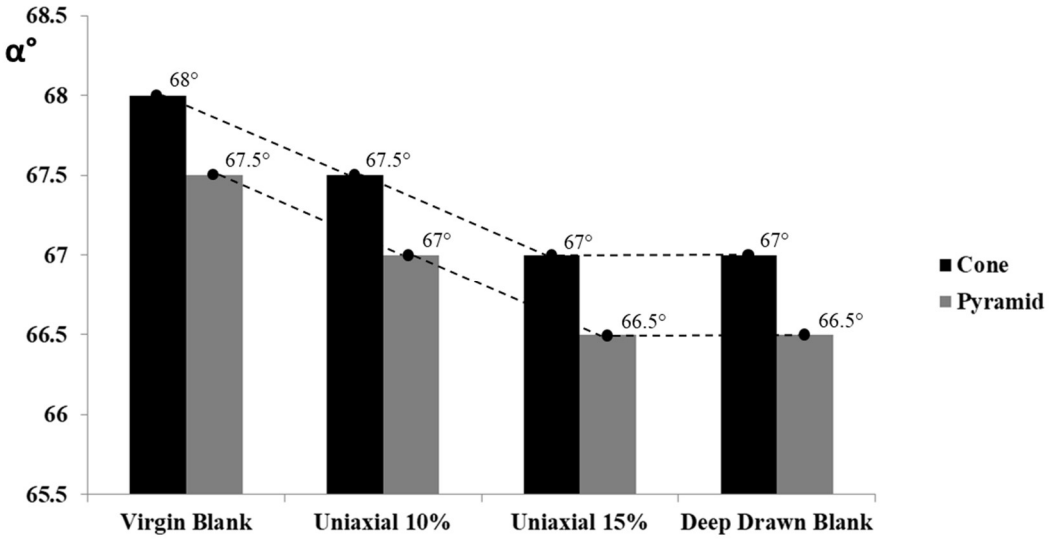

Fig. 6. Obtained α max for different pre-straining levels for both the cone and pyramid case studies.

Furthermore, figure 7 illustrates the right quadrant of the Fracture Forming Limit (FFL) for the two selected case studies under different pre-straining levels. Actually, the reported diagram is an adapted FFL as the strains were measured by performing the SPIF in all the case studies at their respective α max + 0.5°. This approach does not allow to spot any fracture angle occurring between α max and α max + 0.5°, nevertheless for the purpose of this research, in the authors' opinion, such approximation does not affect the conclusions carried out in this section. Actually, such adapted FFL was performed so as to better understand the relation between formability limits in terms of part fracture, as failure by fracture in SPIF occurs without necking or the necking phenomenon is postponed with respect conventional forming processes [35, 36, 37]. Researches proved that large values of r_{part}/r_{tool} and small tool radius r_{tool} lead to failure by fracture with suppression of necking [38], in the same research was proved that in case of necking, the onset of failure is delayed by the stabilizing effects induced by dynamic bending under tension process mechanics. In the present study, a small (4mm) diameter punch was used and no necking was observed. FFL allows a better visualization of the possible reduction in formability of SPIF because of the pre-straining characterizing the starting blank. Strain values measured on the edge of the SPIFed truncated cones and pyramids are presented, strains were measured as close as possible to the identified fracture area. SPIF process applied on a flat sheet with 15% of uniaxial pre-straining and on the deep drawn part lead to the strain values being the same. As expected, the cone case study led to fracture strains conditions close to that of plane strain; in the pyramid case studies a certain amount of minor strain was observed, instead. Overall, it is possible to notice that in all the case studies pre-straining caused a very limited shifting downwards of the FFL. These results confirm the fact that, a good amount of available formability is still present in the parts after their pre-straining.

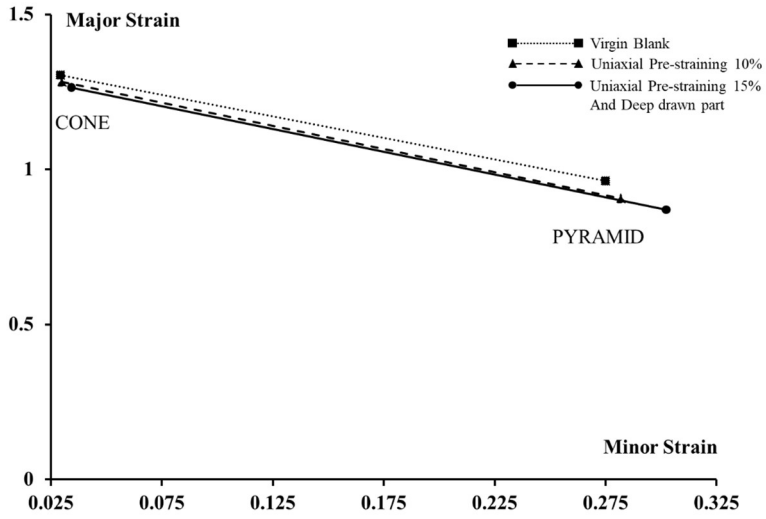

Fig. 7. Adapted Fracture Forming Limits for Virgin and Pre-Strained Blanks for Cone and Pyramid case studies at α max + 0.5°.

4.2 Geometric Accuracy Analysis

All the photo acquired parts were compared to a CAD model corresponding to an ideal part with the same geometry. Some of the results from the geometric analysis are shown in figure 8. The geometric deviation on the lateral sides of the SPIFed shapes has been illustrated for better clarity.

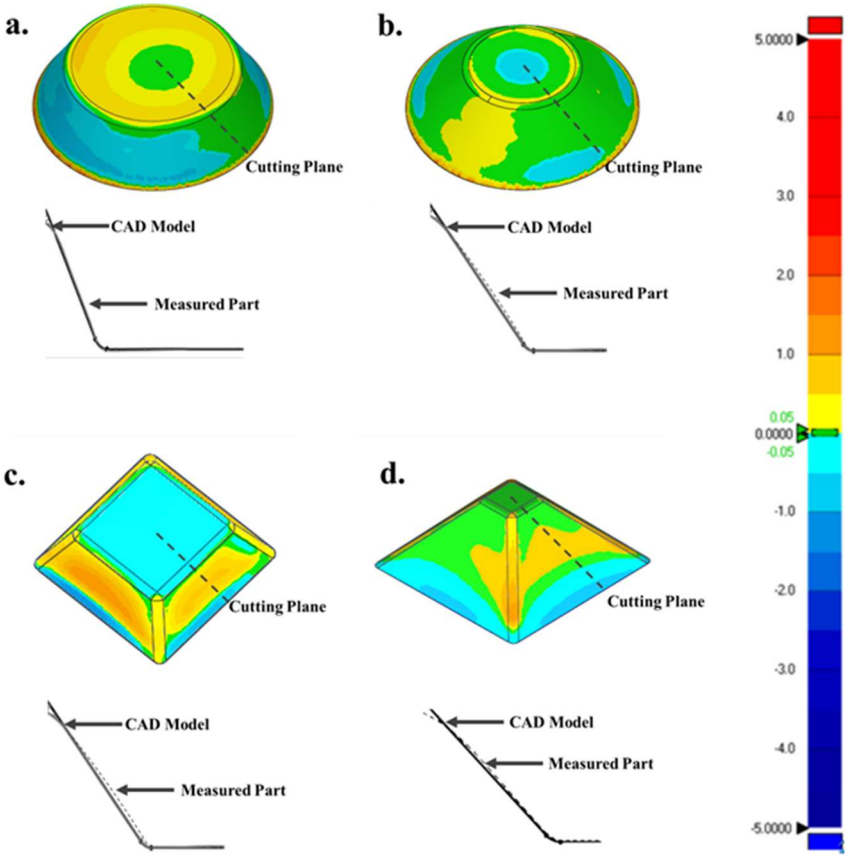

Fig. 8. Geometric Deviation (mm) of scanned parts with respect to CAD geometry corresponding to part IDs: a) 5; b) 3; c) 13; d) 11.

From the analysis, the maximum deviation and the RMS error values were obtained in correspondence to each part's geometrical accuracy. The values have been reported through an Average-Max-Min chart summarizing

the results in the figures 9 and 10 corresponding to the two case studies, respectively. Since three tests were performed for each sample, the scattering indicated the maximum, minimum (indicated with small dots) and the average values (indicated with a big dot), as recorded from the geometric analysis.

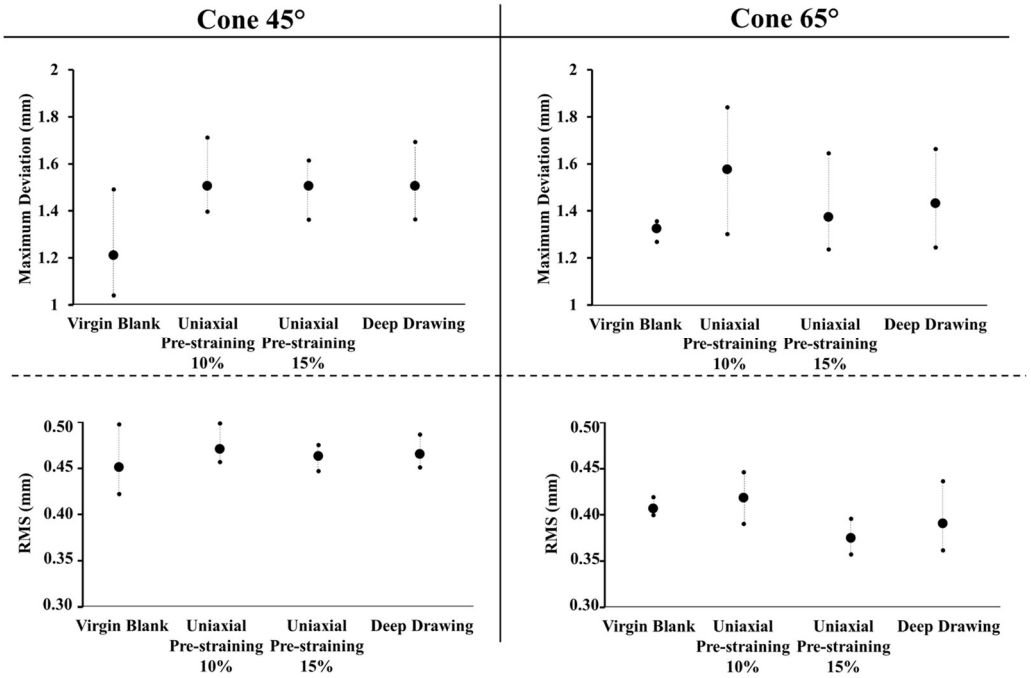

Fig.9. Average-Max-Min chart for geometrical analysis of the Cone case study.

It can be seen that, in the cone case study, fig.9, no clear trend is visible from the obtained data. The geometrical accuracy seemed to worsen with the pre-straining of the parts but no exact correlation can be drawn from the graphs concerning the effect on the level of pre-straining on the accuracy obtained.

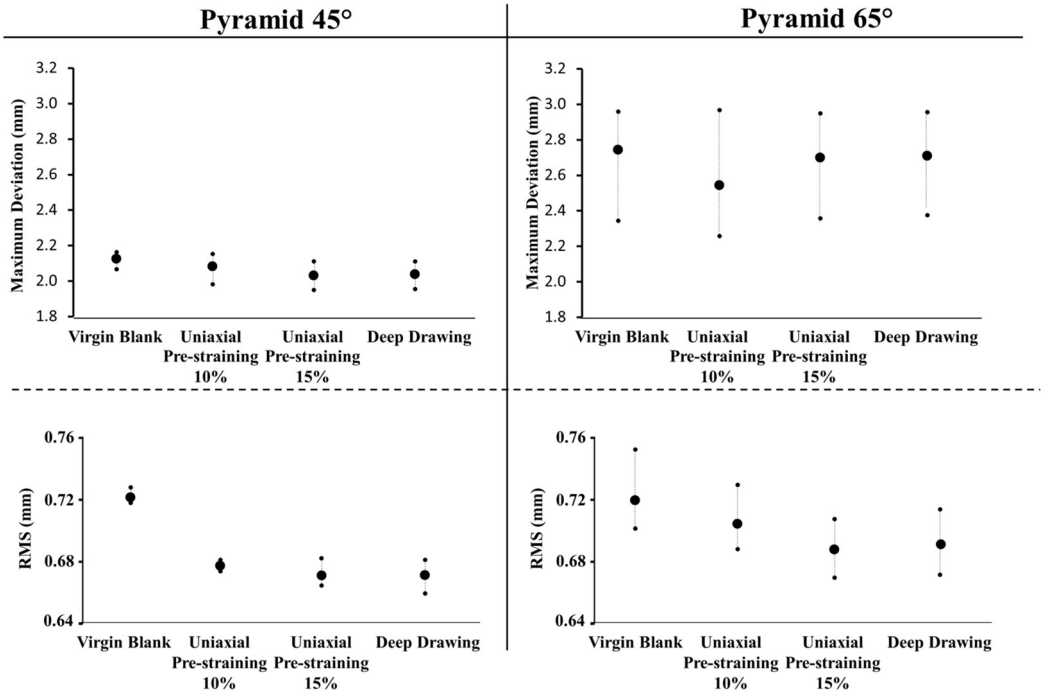

Fig. 10. Average-Max-Min chart for geometrical analysis of the Pyramid case study.

However, in the pyramid case study, fig.10, even an improvement in the SPIF accuracy can be seen with the increase in the pre-straining degrees. With the aim of better understanding the data presented in the graphs and

eventually, derive meaningful interpretations, the ANOVA statistical tool was utilized to clearly identify the influence, if any, of the varying parameters on the geometrical accuracy of SPIF.

4.3 ANOVA analysis

Cone Case Study Figure 11 illustrates the ANOVA analysis results performed on the maximum deviation and the RMS values obtained from the geometric accuracy analysis. The analysis of the maximum deviation values deemed that none of the two factors, Pre-Straining (PS) levels or angles (Angle), resulted as significant ones. Since the obtained p value from the ANOVA analysis was a lot higher than the significance level used during the analysis ($p > 0.05$). On the other hand, the impact of the governing factors on the obtained RMS values of the geometric analysis showed that the selected angle had a significant influence on the RMS values obtained, a P-value of 0.004 paired with the obtained F-value ($F > 3.35$) provides ground for rejecting the null hypothesis (the mean of the Maximum Deviation and RMS for different pre-straining and angles are equal). It is worth noting that, for this case study, the effect of varying the pre-straining levels in either of the two analyzed data was statistically insignificant.

Maximum Deviation

Analysis of Variance for Transformed Response

Source	DF	Adj SS	Adj MS	F-Value	P-Value
Angle	1	0.000027	0.000027	0.03	0.875
PS	3	0.020690	0.006897	7.41	0.067
Error	3	0.002792	0.000931		
Total	7	0.023510			

RMS

Analysis of Variance for Transformed Response

Source	DF	Adj SS	Adj MS	F-Value	P-Value
Angle	1	0.004568	0.004568	62.58	0.004
PS	3	0.000822	0.000274	3.75	0.153
Error	3	0.000219	0.000073		
Total	7	0.005610			

Fig.11. ANOVA analysis results for the Maximum Deviation and RMS values for Cone Case Study.

Pyramid Case Study The results from analyzing the data corresponding to the geometrical accuracy of the truncated pyramid shape via SPIF, are presented in figure 12. From the results it could be concluded that, in case of maximum deviation just the angle resulted as a significant factor influencing the obtained data ($P < 0.05$). Whereas, in the case of RMS data analysis both the factors were relatively significant with the angle having a higher influence on the result, as the corresponding F value was much higher compared to that of pre-straining. Coupling these results with what reported in figure 10 it is possible to state that the pre-straining has a slight beneficial effect on geometrical accuracy. This is phenomenon is due to the fact that the sheet undergoes to strain hardening during the pre-straining and it becomes more rigid. In means that, during SPIF operations, the sheet is less prone to rigid motions, thus, improving the overall geometrical accuracy.

Maximum Deviation

Analysis of Variance for Transformed Response

Source	DF	Adj SS	Adj MS	F-Value	P-Value
Angle	1	0.140566	0.140566	4690.13	0.000
PS	3	0.000192	0.000064	2.13	0.275
Error	3	0.000090	0.000030		
Total	7	0.140848			

RMS

Analysis of Variance for Transformed Response

Source	DF	Adj SS	Adj MS	F-Value	P-Value
Angle	1	0.005131	0.005131	162.40	0.001
PS	3	0.001302	0.000434	13.74	0.029
Error	3	0.000095	0.000032		
Total	7	0.006528			

Fig.12. ANOVA analysis results for the Maximum Deviation and RMS values for Pyramid Case Study.

These results showed that the pre-straining of parts did not have a significant role in affecting the geometrical accuracy of the SPIF process. This deduction points towards the fact the SPIF indeed can be used for the Reshaping of components as the eventual accuracy of parts geometries is highly influenced by the process parameters rather than the pre-straining level the parts underwent prior to their Reshaping. This similar phenomenon as mentioned by Lora et.al. [9] in their work, stating that high levels of pre-straining resulted in

a higher rigidity of the parts, thus, explain the fact that lesser geometrical deviations occur in pre-strained components.

5 Conclusions

This research was aimed at understanding and exploring the use of SPIF process as metal Reuse enabler via the Reshaping approach. The changes in a part's formability and the variation in the achievable shape accuracy through SPIF used as Reshaping process have been analyzed. To achieve this aim, process chains consisting of different types and levels of pre-straining followed by their Reshaping through SPIF were projected, and the resulting α max and final shape accuracy have been determined. Results showed that SPIF though had a reduced formability with the increase in the pre-straining levels, performed decently well for both the analyzed aspects. As a matter of fact, even with a decrease in the formability of SPIF was seen, the difference was minimal and the Reshaping through SPIF could still be performed successfully on the analyzed EoL parts. With regards to the part's geometric accuracy, the ANOVA analysis of the obtained deviation values yielded the conclusion that the pre-straining of the parts, before their Reshaping, did not significantly influence the accuracy performance of SPIF. Rather in some cases increased pre-straining level actually yielded a part with better accuracy in comparison to SPIF performed on a virgin blank. These findings pave the way for future researches which may include further exploration of the considered factors for the Reshaping of metal sheets. The performance of SPIF on sheets with different types of pre-straining should be analyzed.
It is worth remarking that in this paper we assumed that the material properties of pre-strained components are equal to those of EoL components made of the same materials. EoL product recovery entails sheet part disassembly, inspection, de-coating and reshaping are all the steps required to put in place such an approach at industrial scale. De-coating (these processes normally take place at elevated temperatures) could affect the reshaping process, the effect of de-coating step on the mechanical properties and material formability should be further explored. Also, changes in thickness or properties during the use phase could affect the here analysed output (formability and geometrical accuracy).
Finally, the performance of others flexible sheet metal forming processes, such as Hydroforming should be analyzed for exploring the actual potential of the Reshaping approach. Besides the technological issues, research should focus on understanding the industrial scalability of such an approach: identifying proper business models, logistics issues, production planning issues are some of the most important challenges to be still faced.

Declarations

Ethical Approval the Authors Disclose potential conflicts of interest; also the research here presented does not involve neither Human Participants or Animals.

Financial interests: The authors declare they have no financial interests.

Competing Interests: The Authors disclose any financial and non-financial competing interests that could inappropriately influence, or be perceived to influence, this work.

References

[1] Olivetti EA, Cullen JM (2019) Toward a sustainable materials system. Science 360/6396:1396-1398.

[2] International Energy Agency (2019). Material efficiency in clean energy transitions.

[3] Tolio T, Bernard A, Colledani M, Kara S, Seliger G, Duflou JR, Battaia O, Takata S (2017) Design, management and control of demanufacturing and remanufacturing systems. CIRP Annals - Manufacturing Technology 66:585–609.

[4] Li X, Baffari D, Reynolds AP (2018) Friction stir consolidation of aluminum machining chips. The International Journal of Advanced Manufacturing Technology 94(5-8):2031-2042.

[5] Duflou JR, Tekkaya AE, Haase M, Welo T, Vanmeensel K, Kellens K, Dewulf W, Paraskevas D (2015) Environmental assessment of solid state recycling routes for aluminium alloys: Can solid state processes significantly reduce the environmental impact of aluminium recycling? CIRP Annals Manufacturing Technology 64:37–40.

[6] Baffari D, Reynolds AP, Masnata A, Fratini L, Ingarao G (2019) Friction stir extrusion to recycle aluminum alloys scraps: Energy efficiency characterization. Journal of Manufacturing Processes 43:63-69.

[7] Buffa G, Baffari D, Ingarao G, Fratini L (2020) Uncovering Technological and Environmental Potentials of Aluminum Alloy Scraps Recycling Through Friction Stir Consolidation. International Journal of Precision Engineering and Manufacturing-Green Technology 7: 955–964.

[8] Cooper DR, Allwood JM (2012) Reusing Steel and Aluminum Components at End of Product Life. Environmental Science and Technology 46:10334-10340.

[9] Sutherland JW, Adler DP, Haapala KR, Kumar V (2008) A comparison of manufacturing and remanufacturing energy intensities with application to diesel engine production. CIRP Annals - Manufacturing Technology; 57:5–8.

[10] D'Adamo I, Rosa, P. (2016) Remanufacturing in industry: advices from the field. The International Journal of Advanced Manufacturing Technology 86 (9-12): 2575-2584.

[11] Zhang K, Li D, Gui H, Li Z (2019) An adaptive slicing algorithm for laser cladding remanufacturing of complex components. The International Journal of Advanced Manufacturing Technology 101(9-12):2873-2887.

[12] Zhang X, Cui W, Li W, Liou F (2019) Effects of tool path in remanufacturing cylindrical components by laser metal deposition. The International Journal of Advanced Manufacturing Technology, 100 (5-8):1607-1617.

[13] Tilwankar AK, Mahindrakar AB, Asolekar SR (2008) Steel Recycling Resulting from Ship Dismantling in India: Implications for Green House Gas Emissions. Dismantling of Obsolete Vessels 2008; 1-10.

[14] Brosius A, Hermes M, Ben Khalif N, Trompeter M, Tekkaya AE (2019) Innovation by forming technology: motivation for research. International Journal of Material Forming 2:29-38.

[15] Takano H, Kitazawa K, Goto T (2008) Incremental forming of nonuniform sheet metal: Possibility of cold recycling process of sheet metal waste. International Journal of Machine Tools and Manufacture 48:477-482.

[16] Abu-Farha FK, Khraisheh MK (2008) An integrated approach to the Superplastic Forming of lightweight alloys: towards sustainable manufacturing. International Journal of Sustainable Manufacturing 1:18-40.

[17] Ingarao G, Zaheer O, Campanella D, Fratini L (2020) Re-forming end-of-life components through single point incremental forming. Manufacturing Letters 24:132-135.

[18] Zaheer O, Ingarao G, Di Lorenzo R, Fratini L (2021) On the Effectiveness of SPIF Process to Re-Form End-of-Life Components as Compared to Conventional Forming Approach. In Key Engineering Materials 883: 201-208.

[19] Zaheer O, Ingarao G, Pirrotta A., Fratini, L. (2021) Geometrical deviation of end-of-life parts as a consequence of reshaping by single point incremental forming. The International Journal of Advanced Manufacturing Technology, 115(5), 1579-1588.

[20] Ingarao G, Zaheer O, Fratini L (2021) Manufacturing processes as material and energy efficiency strategies enablers: the case of Single Point Incremental Forming to reshape End-of-Life metal components. CIRP Journal of Manufacturing Science and Technology 32:145-153.

[21] McAnulty T, Jeswiet J, Doolan M (2017) Formability in single point incremental forming: A comparative analysis of the state of the art. CIRP Journal of Manufacturing Science and Technology 16:43-54.

[22] Malhotra R, Xue L, Belytschko T, Cao J (2012) Mechanics of fracture in single point incremental forming. Journal of Materials Processing Technology 212:1573–1590.

[23] Silva MB, Nielsen PS, Bay N, Martins PAF (2011) Failure mechanisms in single-point incremental forming of metals. The International Journal of Advanced Manufacturing Technology 56 (9-12):893-903.

[24] Cui Z, Cedric XZ, Ren F, Kiridena V, Gao L (2013) Modeling and validation of deformation process for incremental sheet forming. Journal of Manufacturing Processes 15(2):236-241.

[25] Li Y, Liu Z, Lu H, Daniel WB, Liu S, Meehan PA (2014) Efficient force prediction for incremental sheet forming and experimental validation. The International Journal of Advanced Manufacturing Technology 73(1-4):571-587.

[26] Bansal A, Lingam R, Yadav SK, Venkata RN (2017) Prediction of forming forces in single point incremental forming. Journal of Manufacturing Processes 28:486-493.

[27] Micari F, Ambrogio G, Filice L (2007) Shape and dimensional accuracy in single point incremental forming: state of the art and future trends. Journal of Materials Processing Technology 191(1-3):390-395.

[28] Najm SM, Paniti I. (2021). Artificial neural network for modeling and investigating the effects of forming tool characteristics on the accuracy and formability of thin aluminum alloy blanks when using SPIF. The International Journal of Advanced Manufacturing Technology, 114(9): 2591-261.

[29] Wang C, He A, Weegink KJ, Liu S, Meehan PA (2020) 3D surface representation and trajectory optimization with a learning-based adaptive model predictive controller in incremental forming. Journal of Manufacturing Processes 58:796-810.

[30] Duflou J R, Habraken AM, Cao J, Malhotra R, Bambach M., Adams D., Vanhove H., Amirahmad Mohammadi A., Jeswiet J (2018). Single point incremental forming: state-of-the-art and prospects. International. Journal of Material Forming 11: 743–773.

[31] Lora FA, Fritzen D, Alves De Sousa RJ (2021) Studying Formability Limits By Combining Conventional and Incremental Sheet Forming Process. Chinese Journal of Mechanical Engineering 2021; 34, DOI: 10.1186/s10033-021-00562-7.

[32] Jeswiet J , Young D. (2005) Forming limit diagrams for single-point incremental forming of aluminum sheet Proc Inst Mech Engrs Part B: J Eng Manuf, 219 . 359-364.

[33] Ingarao G, Di Lorenzo R, Micari F(2009) Analysis of stamping performances of dual phase steels: a multi-objective approach to reduce springback and thinning failure, Materials & Design 30(10):4421-4433.

[34] Evans M. Minitab manual. W H Freeman 2009.

[35] Isik K, Silva MB, Tekkaya AE, Martins PAF (2014) Formability limits by fracture in sheet metal forming. Journal of Materials Processing Technology; 214(8):1557-1565.

[36] Jawale K, Duarte JF, Reisa A, Silva MB (2018) Characterizing fracture forming limit and shear fracture forming limit for sheet metals. Journal of Materials Processing Technology 255:886-897.

[37] Soeiro JMC, Silva CMA, Silva MB, Martins PAF (2015) Revisiting the formability limits by fracture in sheet metal forming. Journal of Materials Processing Technology 217:184-192.

[38] Silva MB, Nielsen PS, Bay N, Martins PAF (2011). Failure mechanisms in single-point incremental forming of metals. The International Journal of Advanced Manufacturing Technology,56(9), 893-903.